2020 IEEE/RSJ International Conference on Intelligent Robots and Systems (IROS)
October 25-29, 2020, Las Vegas, NV, USA (Virtual)

Core-centered Actuation for Biped Locomotion of Humanoid Robots*

Caleb Fuller[1], Umer Huzaifa[2], Amy LaViers[3], and Joshua Schultz[1]

Abstract— **In this paper we examine a novel method of core-located actuation that we believe can be used to vary gaits in a compass-gait walker, using critical analysis of a ball-in-tray mechanism to apply forces at the robot's "pelvis". The dynamic equations of motion of a tilting ball-tray system with several design parameters are developed and simulated for various tray designs. Results show that changes in tray design do indeed significantly affect the trajectory. When compared to a hardware ball-tray system, the results show good agreement with the simulation. The sagittal plane component of the ball's trajectory is applied to the motion of a corresponding mass at the "pelvis" of a compass-gait walker. Simulations of the compass-gait walker show that this trajectory generates a feasible gait.**

I. Introduction

Despite recent progress in bipedal walking research, significant hurdles remain. Movement that truly possesses the subtle characteristics of human walking is an area that still needs significant research. There are multiple reasons to use human walking as a tutorial on how to design our bipedal robots some of which are: the stability of human walking, the efficiency of human walking, and the variability of human walking gaits that are adapted to the environment.

Researchers have been pursuing different ways to improve bipedal walking, seeking to improve energy efficiency, stability and simplicity of control algorithms. One significant branch of this research is that of passive-dynamic walking, pioneered by Tad McGeer [1]. He began with a simple planar design that was able to walk stably on an inclined ramp. Later on, Collins and Ruina took this research a step further with their three dimensional passive-walker [2]. Since then researchers have also sought to combine passive walking designs with simple actuation to obtain an efficient walker utilizing clever mechanical design and simple energy input such as Collins and Ruina [3] and Tedrake *et al.* [4].

The method shown in this paper, including a tray mechanism with embedded thin rails where a ball rolls on top, is inspired by a description of human walking from somatic practice, specifically, Bartenieff Fundamentals (BF). BF is a set of principles that describes improving body connections and movement intention [5]. Within BF, a set of six patterning sequences (named the Basic Six), provides a link between the mover's intention and the bodily movements. Three of the Basic Six can be used to describe locomotion: Thigh Lift, Forward Pelvic Shift and Lateral Pelvic Shift.

According to this framework, the movement of the pelvis along the sagittal and lateral axes, creating an oblique shift that *subtly displaces the center of mass*, is a major contributor to locomotion. Moreover, with variation in these elements, a range of walking styles (from a dead end "trudge", to a spritely "stroll") could be obtained by shifting the mass of the core in proper fashion. In addition, findings from biomechanics literature also point out the important role played by different pelvis movements in human walking. For example, in [6], Pelvic Tilt, Pelvic Rotation, and Lateral Pelvic Displacement are identified among the major determining factors for human walking.

Thus, walking, when viewed through the three chosen descriptors from the Basic Six, can be called "core-centered" or "core-located", and we believe that given proper analysis the forces produced by core-located actuation can be used to modulate the gait of a passive-dynamic walker. Initial progress in this vein has been outlined in prior publications [7], [8], [9], [10]. In this paper, we provide experimentally determined core-located shifting motions to a compass gait simulation that result from the natural system dynamics of a heavy ball rolling in a tray equipped with a brushless motor that can set the tray tilt. And by this we show that the simulated ball-tray dynamics are proven accurate such that the theoretical work can be used to determine what design elements are needed for multiple trays in order to attain varieties of gait styles.

The ball provides the energy input that has the potential to drive locomotion of a passive bipedal walker. The tray design leads to different types of gait styles for handling situational walking patterns in social settings, or in specific tasks played out in various environments. This may be advantageous for several reasons: differing gait styles can be more suitable and stable for different walking environments, differing gait styles can give a more comforting perception to humans in the case of human-robot interaction, and differing gait styles can offer variety for different sorts of payloads.

II. Dynamic Model and Ball Tracking Methodl Verification

To produce the perturbations to the biped in a manner similar to how the core muscles do in human walking, we envision placing a heavy ball in a tray that can tilt. In this

*This work was supported by NSF grants 1701378 and 1701295 EAGER/Collaborative Research: Center-of-Mass Control for Expressive and Effective Movement in Bipedal Robots

[1]Caleb Fuller and Joshua Schultz are with Department of Mechanical Engineering, University of Tulsa, Tulsa, OK 74104, USA caleb-fuller@utulsa.edu, joshua-schultz@utulsa.edu

[2]Umer Huzaifa is with the Department of Electrical and Computer Engineering, Rose-Hulman Institute of Technology, Terre Haute, IN 47802, USA huzaifa@rose-hulman.edu

[3]Amy LaViers is with the Department of Mechanical Science and Engineering, University of Illinois at Urbana-Champaign, Champaign, IL 61820, USA alaviers@illinois.edu

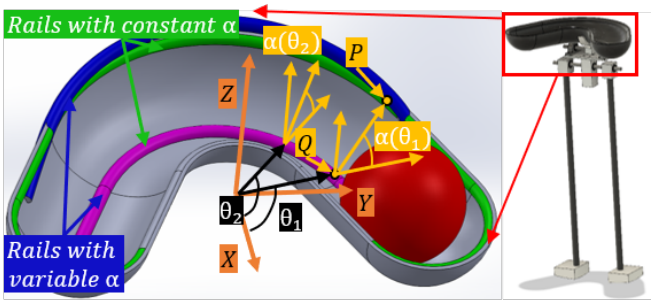

Fig. 1: Pelvic cradle tray design for core-located actuation in a bipedal passive dynamic walker designs. Varying the shape of the tray and the curved profile of the rails that contact the ball changes the system dynamics.

way, the (1.1 kg) ball is driven by the gravitational potential generated by the tilt of the tray, which can be accomplished using an actuator of comparatively modest size (in our case the Anaheim Automation Brushless DC motor with planetary gearbox BLWRPG112s-24v-10000 with a gear ratio of 264:1 was chosen). By studying the equations of motion of the ball in the tray, we can begin to deduce the effect on the passive walker on which it sits. We develop the equations of motion using Lagrangian methods, incorporating the rolling within the tray as Pfaffian constraints, and assuming the tray (which will be light when compared with the ball) is massless.

A. Equations of Motion

The generalized coordinates of the tilting ball-tray system are chosen to be $\boldsymbol{q} = [\theta, \phi]^\top$. θ gives the angular position of a vector in the plane of the tray to the ball's centroid drawn from the center of the radius of the tray as the ball rolls along the path dictated by the tray (see Fig. 1 where two example discrete values, θ_1 and θ_2 are highlighted). ϕ describes the angle of tilt of the tray as it rotates along the axis of rotation (that can be seen in Fig. 2). (Another coordinate, ψ, denotes rotation of the ball about an instantaneous axis between the two rails. The assumption of a no slip condition between the ball and the tray's rails forms a Pfaffian constraint relating $\dot{\theta}$ and $\dot{\psi}$; thus ψ is eliminated in the Lagrangian formulation and does not appear in the equations of motion). $\alpha(\theta)$ is a continuous function that describes the profile of the rails on which the ball rolls (a design parameter). Under these constraints and assumptions, the rolling of the ball is described by the following equations of motion, where M_{ij} are the elements for the mass matrix $\boldsymbol{M}$, C_{ij} are the elements of the matrix $\boldsymbol{C}$ representing the coriolis and centripetal acceleration terms, and G_{ij} are the elements of the gravity matrix $\boldsymbol{G}$:

$$\boldsymbol{M}(\boldsymbol{q})\ddot{\boldsymbol{q}} + \boldsymbol{C}(\boldsymbol{q}, \dot{\boldsymbol{q}})\dot{\boldsymbol{q}} + \boldsymbol{G}(\boldsymbol{q}) = \begin{pmatrix} 0 \\ \tau \end{pmatrix} \tag{1}$$

$$\begin{aligned} M_{11} &= mR^2 \frac{(R_B^2 + K^2 R \sec(\alpha(\theta))^2)}{R_B^2} \\ M_{12} = M_{21} &= -mR \frac{(K^2 + hR_B)\sin(\theta)}{R_B} \\ M_{22} &= m(h^2 + K^2 + R^2 + 2R^2\cos(\theta) + R^2\cos(\theta)^2) \end{aligned} \tag{2}$$

$$\begin{aligned} C_{11} &= K^2 mR^2 \frac{\sec(\alpha(\theta))^2 \tan(\alpha(\theta))\alpha`(\theta)}{R_B^2} \\ C_{12} &= mR^2(1+\cos(\theta))\sin(\theta) \\ C_{13} &= 0 \\ C_{21} &= -mR\frac{(K^2 + hR_B)\cos(\theta)}{R_B} \\ C_{22} &= 0 \\ C_{23} &= -mR^2 \csc(\frac{\theta}{2})^2 \sin(\theta)^3 \end{aligned} \tag{3}$$

$$\begin{aligned} G_{11} &= -mR\sin(\theta)\sin(\phi) \\ G_{21} &= m\frac{RR_B\cos(\phi) + RR_B\cos(\theta)\cos(\phi) - hR_B\sin(\theta)}{R_B} \end{aligned} \tag{4}$$

Table I lists the design constants appearing in equations 1-4. Equations (1)-(4) are simulated using Wolfram Mathematica to numerically solve for the motion of the ball as it rolls along the tray. Using the simulation results we are able to determine what movements of the ball are ideal for generating certain gait styles as outlined in Huzaifa *et al.*'s previous work [9] and select tray designs and tilting motions that will generate them.

TABLE I: System Constants

Constraint	Description
R	radius of tray curve
$R_{straight}$	calculated radius of straight section
h	offset height, axis of rotation to centroid of ball
R_B	radius of ball
m	mass of ball
K	radius of gyration of ball

B. Ball tracking using OPENCV

In order to track θ over time and compare it with the simulated value we used the open source tool OPENCV and a commercial webcam (Microsoft Kinect v1 360) along with an algorithm that accounts for rotation ϕ of the tray. The algorithm used for tracking the ball uses a pinhole camera model and established concepts in the realm of computer vision and object tracking, along with geometric relationships and known parameters of the tray.

Tracking the ball in the image started with masking the image for the color of the ball and then finding the largest contour in the resulting binary image mask. The centroid of the minimum circumscribing circle of the largest contour

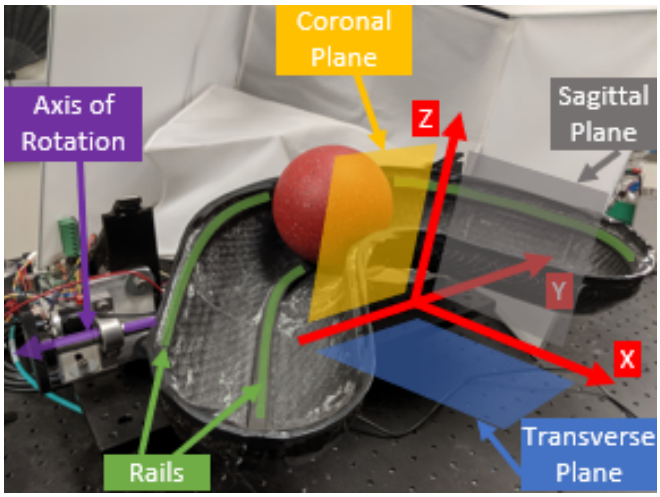

Fig. 2: Carbon fiber tray with candlepin bowling ball rotating along an axis driven by a brushless motor made by Anaheim Automation and a RoboteQ SBL series motor controller.

was taken to be the pixel corresponding to the center of the ball in the image. We combined the recorded image pixel history (corresponding to the ball centroid in the image) with knowledge of the distance to a fixed point of reference in the picture (the axis of rotation), and then used geometric relationships and known tray geometry along with the recorded tray tilt motor's hall sensor data (giving us the value of ϕ and therefore describing the plane of the tray at each instant in time) to determine the corresponding angle θ describing position of the ball. θ, ϕ and the tray geometry allow us to reconstruct the ball centroid's position in $\mathbb{R}^3$.

In Sec. V, we compare this measured θ with that returned by the dynamic model (1)-(4) that we have derived. The measured time history of the hall sensors of the DC motor is supplied to the simulation as an input.

III. Ball-Tray Hardware Design

The proposed design is a "V"-shaped tray with corner fillet in which a heavy ball rolls along the track determined by the tray (see Fig. 2). The system was designed so that it would give shifting of a core mass in both the lateral directions in the frontal/coronal plane and forward-backward directions in the sagittal plane. This gives the ability to create a variety of movement paths in 3-dimensional space by using trays of differing shapes, different curved profiles of the rails and varying the tray tilt during the gait.

The profile of the tray dictates the movement of the mass which is acting as the main instrument of energy input to the system. Therefore, taking care to consider *how a particular shape can reinforce or arrest the motion of the compass gait of a biped is the goal of the tray hardware development.* The main parameters that we can consider in the tray design are: the radius of curvature of the tray and the angle between the rails upon which the ball is rolling (this is discussed in more detail in Sec. IV, and is portrayed in Fig. 3b).

The tray was formed from carbon fiber composite, which has a high strength to weight ratio and can be molded to the custom shapes required in this experiment. The tray was manufactured using a typical two step carbon fiber layup process, 1) the casting of the mold, and then 2) the carbon fiber layup itself.

IV. Variable Paths of Movement

The key advantage of this hardware design is that a change to any of the parameters that govern the dynamic behavior is readily transmitted to a new tray geometry through this manufacturing process. Changes to the hardware design manifests itself by a change in the ball-tray dynamics and in turn, a change in the walking gait of the biped.

One of the most interesting design elements of the tray rests with the angle $\alpha(\theta)$ between the rails of the tray, see Fig. 3a. This is easily modified in the CAD model of the mold. The best way to understand this feature and how it affects the motion of the ball-tray system is to look at the first term of both the mass matrix and the centripetal/Coriolis matrix $\mathbf{C}$, see equations (2) and (3). One can see that as this angle changes throughout the curve of the tray it offers subtle changes in the dynamics of the tray.

This is in some respects a curved-path analog to the popular game "Shoot the Moon", in which the goal is to bring a metal ball as far up the game board as possible (under gravity) while it rolls on two rails. The player moves the rails apart or closer together, which changes the contact points on the metal ball, thus affecting the rolling motion while trying to avoid dropping the ball prematurely. The dynamics associated with this motion (with straight rails moved by the player) was analyzed by Xu, Groff, and Burg [11].

Fig. 3b shows the simulation result of $\theta(t)$ given tray tilt(ϕ) vs. time corresponding to the "Input Signal" function used in the experiment (whose results are pictured in Fig. 3d), using three different examples of $\alpha(\theta)$ and one change in radius. The first is simply a constant value of α for all θ, the second and third plotted curves, are scaled $\cos$ functions of θ, and the last shows a constant value of theta but a larger radius of the tray. This plot is interesting because it exhibits significant variability of the ball trajectory, and the function $\alpha(\theta)$ can be selected based upon the desired walking gait of the biped.

V. Experimental Results

Figs. 3c-3d show plots of θ captured experimentally against θ from simulation when given the same input signal, ϕ, that was captured from the hall sensor of the motor driving the system. The data from these experiments shows satisfactory agreement. The model diverges from the experiment in some places (more telling in Fig. 3d which shows more transient features of the movement), but not to a degree that limits the usefulness of the model in making design decisions. Despite small errors between simulation and experiment, they are close enough that the model can be used for predicting what type of core-centered motion is desired to produce a certain walking gait. This deviation

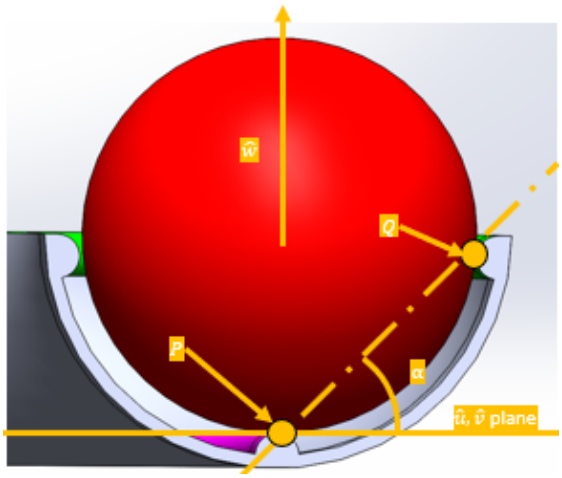

(a) the angle α of the line joining the contact points at each $\theta(t)$

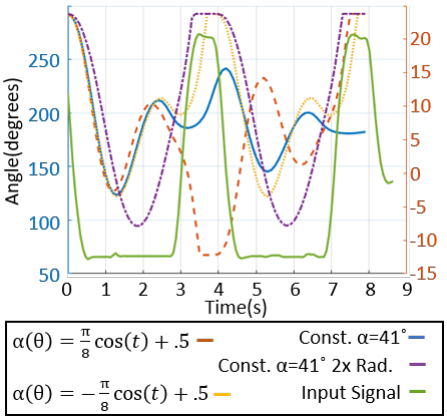

(b) simulated ball trajectories with different $\alpha(\theta)$

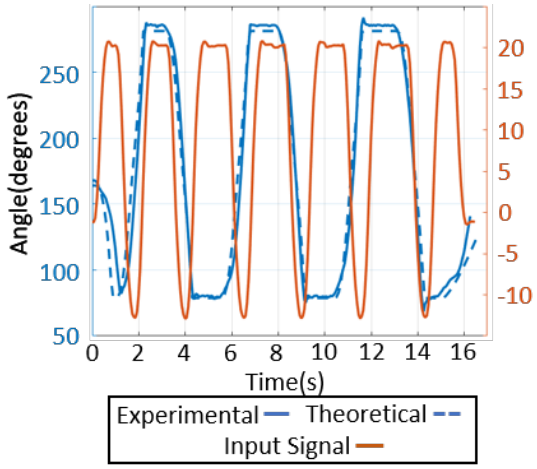

(c) ball moves from end to end of tray

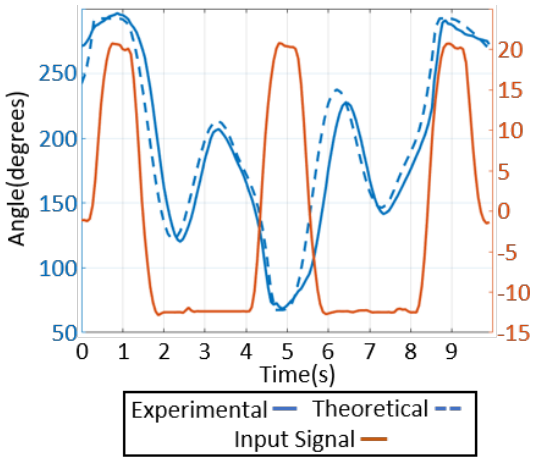

(d) tray reciprocates before the ball reaches the end

Fig. 3: Modifying the parameters governing the shape of the tray changes the system dynamics of the rolling of the ball, which could later be used to tune walking gaits. (a) shows the angle α between the tray's rails, which can vary continuously with ball excursion θ. (b) shows three radically different trajectories resulting from the same tray tilt profile when different functions are chosen for $\alpha(\theta)$, or a different radius is used. (c) and (d) show the simulation result for the tray in Fig. 2 compared against the trajectory measured using the camera, first where the tilt profile moves the ball from one end to the other, and a second where the changing tilt causes the ball to reverse direction before completing the cycle.

likely occurs due to the limitations of the viscous damping model used to account for rolling resistance and artifacts from the vision tracking of the ball. Based on this level of agreement, we believe that the parameters (R, α) selected from the simulation will produce the same effect in the physical hardware.

Initial attempts at matching the model to the experiment showed that rolling resistance could not be ignored and thus a simple viscous damping term was added to Eq. 1, $\begin{pmatrix} 0 \\ c \end{pmatrix} \dot{\theta}$

The c used in simulation was characterized experimentally by releasing the ball from rest with the tray at $\phi = const.$ and choosing the c that best represented the trajectory observed. The resulting value was used in all subsequent simulations.

VI. Examining the Tray Mechanism as a Pelvis-Inspired Actuator for Biped Models

The hardware tray mechanism as discussed can provide a method of shifting the center of mass using reasonably small and low power actuators adjacent to the center of mass of the robot. As discussed in Sec. I, the core provides a similar functionality in human walking according to the Basic Six. We have employed the experimental shift in the center of mass using this mechanism to examine whether this can lead to a feasible gait in a previously constructed three-link planar biped model simulation. We can examine the effect that this tray motion will have inserting the trajectory of the ball found in the experiment into the biped with core mass simulation framework developed as part of our prior work[9]. This amounts to setting the simulation parameter

PS in that environment (summarized below) according to the ball trajectory measured. This had previously been set as the result of a numerical search to identify promising gaits, without being generated by a physical mechanism.

The biped model (in summary) consists of a modified compass walker [12] with an actuated leg and a mass at the "hip" allowed to move forward and backward (as if moved by a high-power, high-bandwidth virtual prismatic actuator), achieving a similar effect to the Forward Pelvic Shift from the Basic Six. The biped model can be described using *its own* set of generalized coordinates: $\boldsymbol{q_s} = [q_{st}, q_{sw}, d_t]^T$, where, q_{sw} represents the absolute angle of the swing leg, q_{st} gives the absolute angle of the stance leg, and d_t shows the displacement of the pelvis mass M_t from the hip. The corresponding state vector is $\boldsymbol{x_s} = [q_{st}, q_{sw}, d_t, \dot{q}_{st}, \dot{q}_{sw}, \dot{d}_t]^T$. A comprehensive description of this model is found in [13].

The gait generation for this model is carried out by solving a feasibility problem formulation in which state $\boldsymbol{x_s}(t)$ and input $\boldsymbol{u}(t)$ vectors are determined such that they satisfy the constraints for walking (also covered in a previous paper by Huzaifa and LaViers [10]). The constraints on the feasibility problem are: the dynamics of the biped model (given by inertia matrix $\boldsymbol{D_s}$, Coriolis/centripetal matrix $\boldsymbol{C_s}$ gravitation matrix $\boldsymbol{G_s}$, and generalized forces vector $\boldsymbol{\Gamma_s}$); that the normal ground reaction force on the stance foot, $F_N^{st}(t)$, must be positive; that the ratio of the ground reaction forces must lie in the friction cone, satisfying: $|\frac{F_N^{st}(t)}{F_T^{st}(t)}| \leq \mu$, where μ is the coefficient of friction for the walking surface; and the desired trajectory for d_t be defined by the gait parameter, **PS**. The constraints which are satisfied at the end points of a walking step (corresponding to time instants $t = 0$ and $t = t_f$) are: the step length constraint defined by the gait parameter, **TL**; and a periodicity constraint at the end of the walking step (defined by the impact map Δ of leg impact with the ground). Using these constraints, the feasibility problem is as follows:

$$
\begin{aligned}
\min_{\boldsymbol{u}(t)} \quad & J(\boldsymbol{u}(t)) = 100 \\
\text{s.t.} \quad & \dot{\boldsymbol{x}}_{\boldsymbol{s}} = \boldsymbol{D_s}^{-1}(-\boldsymbol{C_s}\dot{\boldsymbol{q}}_{\boldsymbol{s}} - \boldsymbol{G_s} + \boldsymbol{\Gamma_s}) \\
& F_N^{st} > 0,\ F_T^{st} < \mu F_N^{st} \text{ and } F_T^{st} > -\mu F_N^{st} \\
& r(\sin(q_{st}(t_f)) - \sin(q_{sw}(t_f))) = \mathbf{TL} \\
& r(\cos(q_{st}(t_f)) - \cos(q_{sw}(t_f))) = 0 \\
& ||d_t - d_t^{des}(\mathbf{PS})||^2 = 0 \\
& \boldsymbol{x_s}(0) = \Delta(\boldsymbol{x_s}(t_f)) \\
& x_{s_{min}} \leq \boldsymbol{x_s} \leq x_{s_{max}} \\
& u_{min} \leq \boldsymbol{u} \leq u_{max} \\
& t \in [0, t_f]
\end{aligned}
\tag{5}
$$

Since the objective function J is a constant, the above minimization searches for a feasible solution satisfying the given constraints, for the chosen values of **TL** and **PS**. The biped model parameters and the range of values for state and input vectors are given in Table II.

For finding the solution in Eq. 5, the initial and final states in the state trajectory are initialized to:

$$x_s(0) = [-0.17, 0.34, 0.25, 1.45, 0.53, -0.39],$$
$$x_s(t_f) = [0.34, -0.17, 0.25, 1.66, -3.25, -0.42].$$

The solution to the above problem is obtained by using the optimization toolbox GPOPS II [14] and is run on a laptop computer running a 2.2 GHz Core i7 processor. The code is written in MATLAB using the toolbox in [15], which leverages direct collocation [16].

TABLE II: Range of input and state vectors, and values of model parameters, used in the optimization problem Eq. 5 for finding gaits of the given biped model.

Symbol	Name	Value or Range of Values (lower limit, upper limit)
u_1	Swing Leg Torque	$(-100, 100)$ Nm
u_2	Force on Pelvis Mass	$(-100, 100)$ N
$[q_{st}; q_{sw}]^T$	Leg Joint Angles	$[(-\frac{\pi}{2}, \frac{\pi}{2}); (-\frac{\pi}{2}, \frac{\pi}{2})]^T$
d_t	Displacement of Pelvis	$(-0.1, 0.5)$ m
$[\dot{q}_{st}; \dot{q}_{sw}]^T$	Joint Angle Velocities	$[(-5, 5); (-5, 5)]^T$ rad/s
$\dot{d}_t$	Velocity of Pelvis	$(-5, 5)$ m/s
M_t	Pelvis mass	1.089 kg
m	Mass of each leg	0.544 kg
r	Length of leg	1 m

A. Driving the biped simulation using the tray input

Using the above mentioned framework, we have explored using the tracked position data of the ball to define the gait variable **PS** for generating a corresponding gait in our biped model. Since the tray on which the ball rolls is assumed to be massless in comparison to the ball, the position data can be assumed to represent the position of the center of mass of the moving core.

For use in the planar biped model, we took the x component of the ball position atop the tray (also displayed in Fig. 4a). From the data obtained in the tray experiment (shown by blue markers in Fig. 4a), points for one round trip of the ball between the two ends of the tray (shown by red markers in the following figure) were selected, for which a range of feasible gaits can be generated. A 5^{th} order polynomial was fit to the extracted data points (plotted against the data points in Fig. 4b) using a built-in MATLAB function, `fit`, to define the desired path (**PS**) for the core mass in the biped model.

By using the curve in Fig. 4b as **PS** in the problem formulation Eq. 5, a range of feasible gaits has been found for $0.01 \leq$ **TL** ≤ 0.45. Individual waveforms for joint position $q_s(t)$ and input variables $u(t)$ corresponding to **PS** curve and **TL** $= 0.3$ and "frames" of the gait are provided in Figs. 4c and 4d, respectively.

The fact that the gait corresponding to the **PS** obtained from the hardware mechanism is feasible indicates that the hardware mechanism may provide the necessary shift in the center of mass as observed in humans for walking. If installed as a core-inspired actuator that sits on top of a two-legged walker, it can introduce disturbances along the sagittal and lateral axes, and the legs may adjust to these dynamic actions while taking a step. This scheme would contrast with currently-favored actuation strategies used in

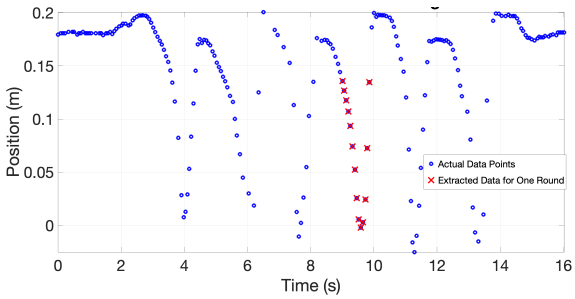

(a) actual trajectory of the ball (sagittal plane component)

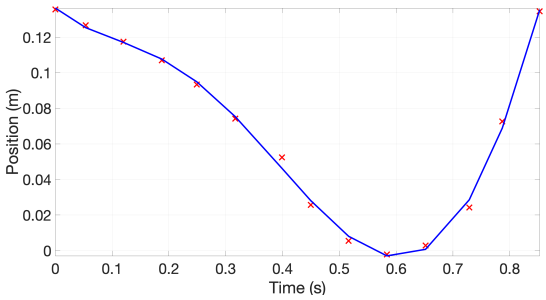

(b) polynomial fit to define **PS** for the gait in Eq. 5

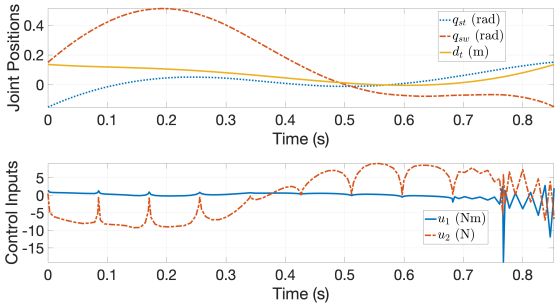

(c) time history of gait coordinates with this **PS** as an input

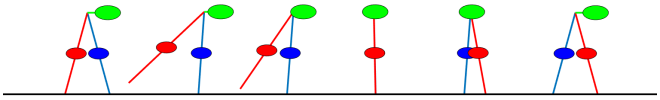

(d) frames from resulting compass gait animation

Fig. 4: Experimental position data (obtained as discussed in Sec. II) showing six cycles of the ball from one end of the tray to the other (a). Points from a single cycle are extracted to define a desired path (**PS**) for pelvis mass in the biped simulation by fitting a 5th order polynomial to the points (b). This **PS** is used to find a corresponding feasible gait in the biped simulation, illustrated in (c) and (d).

humanoids and bipedal robots where the actuation occurs away from the robot's center of mass (e.g., in hips, knees, and ankles) and may provide more agility while walking, better imitating human locomotion performance.

VII. Conclusion

This paper has proposed and validated a dynamic model of a ball-tray system that in future work we hope to set atop a bipedal walker, providing perturbations to the walker similar to the actions of the human core when walking. Simulations indicate that changing the tray geometry and tilt profile changes the time history of these perturbations significantly. In addition, when experimentally collected ball trajectory data is applied to the simulation of a compass gait walker, the tray actions lead to a feasible gait. This lends credence to the idea that a specific desired gait can be invoked by varying the tray parameters and the tray tilt vs. time as an alternative to large actuators in the "knees" and "hips" of the walker. Future work will evaluate additional combinations of tray parameters, searching for those that correspond to specific gait styles identified by human experts. Additional simulations will be developed that include the coupling between the tray dynamics and the gait dynamics with greater fidelity. A human-scale biped will be constructed to validate the performance of the complete system as a means of generating variable gait styles.

References

[1] T. McGreer, "Dynamics and Control of Bipedal Locomotion," *Theoretical Biology*, no. 163, pp. 277–314, 1993.

[2] S. H. Collins, M. Wisse, and A. Ruina, "A Three-Dimensional Passive-Dynamic Walking Robot with Two Legs and Knees," Tech. Rep. 7, 2001.

[3] S. H. Collins and A. Ruina, "A bipedal walking robot with efficient and human-like gait *," in *Proceedings of the 2005 IEEE International Conference on Robotics and Automation*, 2005, pp. 1983–1988.

[4] R. Tedrake, T. W. Zhang, M.-F. Fong, and H. S. Seung, "Actuating a Simple 3D Passive Dynamic Walker," in *IEEE International Conference on Robotics and Automation*, New Orleans, 2004.

[5] K. Studd and L. Cox, *Everybody is a Body*. Dog Ear Publishing, 2013.

[6] S. Mochon and T. A. McMahon, "Ballistic walking," *Journal of Biomechanics*, no. 1, pp. 49–57, 1980.

[7] U. Huzaifa, C. Bernier, Z. Calhoun, G. Heddy, C. Kohout, B. Libowitz, A. Moenning, J. Ye, C. Maguire, and A. LaViers, "Embodied movement strategies for development of a core-located actuation walker," in *Proceedings of the IEEE International Conference on Biomedical Robotics and Biomechatronics*, 2016.

[8] U. Huzaifa and A. LaViers, "Control design for planar model of a core-located actuation walker," in *Proceedings of the IEEE International Conference on Biomedical Robotics and Biomechatronics*, 2016.

[9] U. Huzaifa, C. Fuller, J. Schultz, and A. LaViers, "Toward a bipedal robot with variable gait styles: Sagittal forces analysis in a planar simulation and a prototype ball-tray mechanism," in *IEEE/RSJ International Conference on Intelligent Robots and Systems (IROS)*, 2019.

[10] U. Huzaifa, C. Maguire, and A. LaViers, "Toward an expressive bipedal robot: Variable gait synthesis and validation in a planar model," *International Journal of Social Robotics*, Apr 2019.

[11] P. Xu, R. Groff, and T. Burg, "The Rigid Body Dynamics of Shoot-the-moon Game and Model-based Controller Design," in *American Control Conference*, 2010.

[12] A. Goswami, B. Espiau, and A. Keramane, "Limit cycles in a passive compass gait biped and passivity-mimicking control laws," *Autonomous Robots*, vol. 4, no. 3, pp. 273–286, 1997.
[13] U. Huzaifa and A. LaViers, "Control design for planar model of a core-located actuation walker." in *IEEE BioRob*, 2016.
[14] M. A. Patterson and A. V. Rao, "Gpops-ii: A matlab software for solving multiple-phase optimal control problems using hp-adaptive gaussian quadrature collocation methods and sparse nonlinear programming," *ACM Transactions on Mathematical Software (TOMS)*, vol. 41, no. 1, p. 1, 2014.
[15] M. P. Kelly. OptimTraj User's Guide, Version 1.5.
[16] J. T. Betts, *Practical Methods for Optimal Control and Estimation Using Nonlinear Programming*, 2nd ed. New York, NY, USA: Cambridge University Press, 2009.